JOURNAL OF AERONAUTICAL MATERIALS
Vol. 42, Issue-05, 2022
pp.142-151

EXPERIMENTAL ANALYSIS OF WAAM OF ER4043-ALN COMPOSITE FOR THE AUTOMOTIVE INDUSTRY

P. Kumar[1], A. Mahamani[2], B. Durga Prasad[3]

[1,3]Department of Mechanical Engineering, Jawaharlal Nehru Technological University Anantapur, Ananthapuramu 515002, Andhra Pradesh, India

penumurukumar.pk@gmail.com

[2]Department of Mechanical Engineering, Sri Venkateswara College of Engineering and Technology, R V S Nagar, 517127, Andhra Pradesh, India

Abstract

Wire Arc Additive Manufacturing (WAAM) has received extensive interest from academics owing to its ability to produce engineering components in large quantities at a low cost with minimal material waste. MIG welding-based wire and arc additive manufacturing using ER4043 filler wire with AlN reinforcing ratios of 0%, 2.5%, 5% and 7.5% were deposited in longitudinal and transverse directions in layers. The WAAM parts are examined by using scanning electron microscopy demonstrating that AIN reinforcement was present despite material loss under all test circumstances. The engine block, cylinder liners, and pistons are just a few of the places where the produced composite may be put to use.

Keywords: Wire Arc Additive Manufacturing, composites, SEM, AlN, Hardness.

1. Introduction

Wire Arc Additive Manufacturing (WAAM) is a technique that was created from arc welding and is particularly well suited for producing big components due to its rapid deposition rates, affordable equipment and feedstock costs and ability to produce complex geometries. Using an arc, the wire is heated and then melted in WAAM. Once in a pool of liquid metal, the convecting droplets are transferred. The pool's surface deforms due to the liquid metal being pushed around by a surface tension gradient. The moulds are subsequently filled with the hardened molten pool [i ii iii iv v]. Aluminium and its alloys are widely used due to their exceptional mix of properties. This is because they are light in weight, thermal and electrically conductive, and strong. A passivating oxide layer protects aluminium alloys from corrosion, weathering, and a corrosive environment [vi vii]. Producing complicated metal components consisting of alloys of aluminium, titanium, and nickel has been a major focus in recent years. Aluminium is critical for the mass manufacture of lightweight components due to its cheap cost and material qualities. Subtractive manufacturing processes such as milling or turning hit their technological limitations regarding the maximum accessible area or undercut creation in complicated components. Additionally, this leads to a large chip volume, which affects the process's efficiency [viii].

However, WAAM is restricted by flaws such as porosity and solidification fractures in aluminium materials [ix x]. The primary issue is porosity, which significantly limits the

mechanical qualities of components, such as strength and ductility [xi xii xiii xiv]. Additive manufacturing creates metal layer by layer, unlike single-pass welding. This influences the formation of pores, particularly in age-hardenable aluminium alloys [12]. Phosphorus in aluminium depends on the arc welding operation, process factors such as welding speed and the consequent heat input [9, 11, xv xvi]. Additionally, porosity is influenced by other parameters such as wire quality and alloy composition [xvii xviii], as well as interpass temperature [xix xx xxi], and is dependent on the microstructure being created [11, xxii xxiii]. Hamilton et al. [xxiv] described a cryomilling-enabled mechanical alloying system to prepare the mixture of aluminium and TiC powder feedstock for the additive manufacturing process. The result shows that the powder feedstock has a uniform distribution of the TiC throughout the aluminium powder. Chen et al. [xxv] fabricated Al-Al composites via the nitrogen-bearing gas bubbling method, and Fale et al. [xxvi] fabricated the same composites using the melt metallurgy technique. During the WAAM, the deposition direction of filler significantly influences microstructure and mechanical properties. An anisotropy study on the mechanical properties of the WAAM samples is described by Zhang et al. [xxvii]. The augmented vibration decreases the porosity of both longitudinal and transverse samples, thereby improving the mechanical properties.

As can be seen from the preceding discussion, there have been many studies on the wear behaviour of MMCs, but there is still a need for a more nuanced understanding of the role that reinforcement plays in the material's enhanced resistance to wear. This study used a pin-on-disk wear testing unit to analyze the factors that influenced the wear of ALN particles embedded in a composite of aluminium and nickel at reinforcement levels of 0%, 2.5%, 5%, and 7.5%. The quality of the samples prepared was verified with microstructure evaluation followed by SEM analysis and microhardness.

2. Experimentation

The substrate was a commercial aluminium alloy 6061 plates with dimensions of 200 X 150 X 15mm, and the components were deposited using ER4043 aluminium alloy wire with a diameter of 1.2mm [xxviii]. Table 1 shows the alloy and wire's chemical makeup. To obtain a stable molten pool over the substrate with adequate size wire feeding, arc current and arc length are set at 1.5m/min, 150A and 3.5mm respectively. Multilayer deposition substrate whose weldability assures layer stability. The interpass temperature is maintained between the passes below 150ºC to avoid cold cracking [22]. The quality of the beads is evaluated with visual inspection and found to be crack-free. The flange is built up of a total of 7 layers that are stacked in both X and Y directions and have an 8mm bead height. AlN particles were blended with 100% ethanol before being coated with an identical weight percentage between layers. The WAAM samples are fabricated under different reinforcement ratios such as 0 %, 2.5 %, 5% and 7.5 %, as illustrated in Figure 1. The wire feed speed (WFS) of ER4043 was tuned using equation (1) to attain identical AlN element composition.

$$E = \frac{\sum WFS_i D_i^2 \rho_i E_x}{\sum WFS_i D_i^2 \rho_i} \qquad (1)$$

Where Ex is the amount of element x in a given wire, WFS_i (i=1, 2) is the wire feed speed, D_i is the wire's diameter, and ρ_i is its density. Compositional data of the key components were both estimated and verified using an inductively coupled plasma OES.

Table 1. Chemical composition of the substrate and the welding wire (wt %).

Material (Function)	**Si**	**Fe**	**Cu**	**Mn**	**Mg**	**Zn**	**Ti**	**Al**
Substrate	0.62	0.33	0.28	0.06	0.9	0.02	0.15	Remainder
Filler wire	4.5	0.8	0.3	0.05	0.05	0.1	0.2	Remainder

The wall constructs under investigation are shown in Figure 1, with a maximum length of about 180 mm and a minimum height of about 110 mm, and they were made using an alternating building approach. We used a band saw to cut away the substrate. All the remaining wall sections were milled down to a uniform thickness. After that, specimens were taken both in the buildup direction (vertical) and the welding direction to analyze the microstructure, hardness, and wear (horizontal). Microstructure and geometric property examination required grinding and polishing of samples, as shown in Figure 2. Barker asserts that electrolytic etch polishing and etching were used to investigate the microstructure. Further, the composite samples are machined and made cylindrical for conducting a pin-on-disk wear test, as shown in Figure 3.

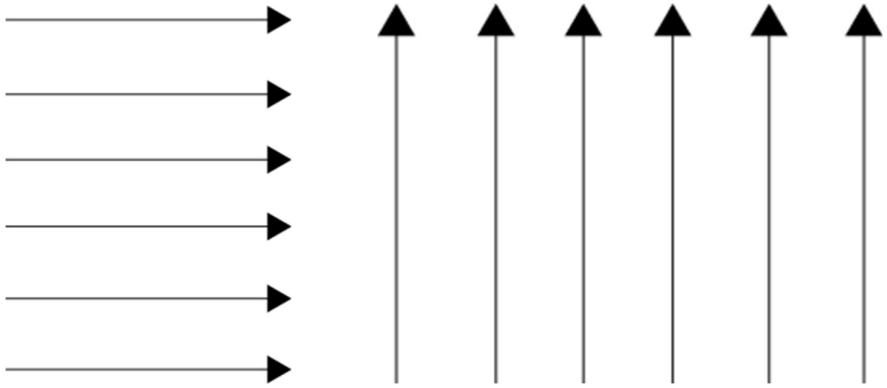

Figure 1 Orientation used for the experimentation

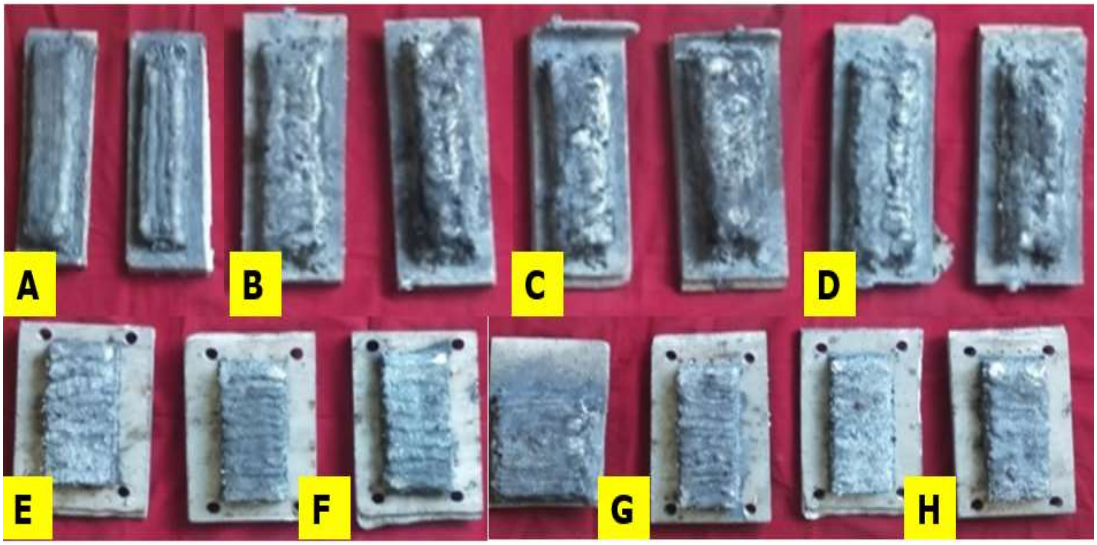

Figure 2 Samples prepared from the WAAM process with different reinforcement ratios.

3. Results and discussion

3.1. Microstructure and energy dispersive analysis

A disc polishing machine was used to polish the specimens to 1200-grit SiC paper and then to 6, 3, and 0.5-grit diamond pastes. Microstructures were recorded using an optical scanner after polishing specimens of weld joints with sodium hydroxide (NaOH) and potassium permanganate (KMnO4), and then etched with the color etchant. The scanning electron micrographs of the ER4043-AlN composites are recorded and displayed in Figure 4.

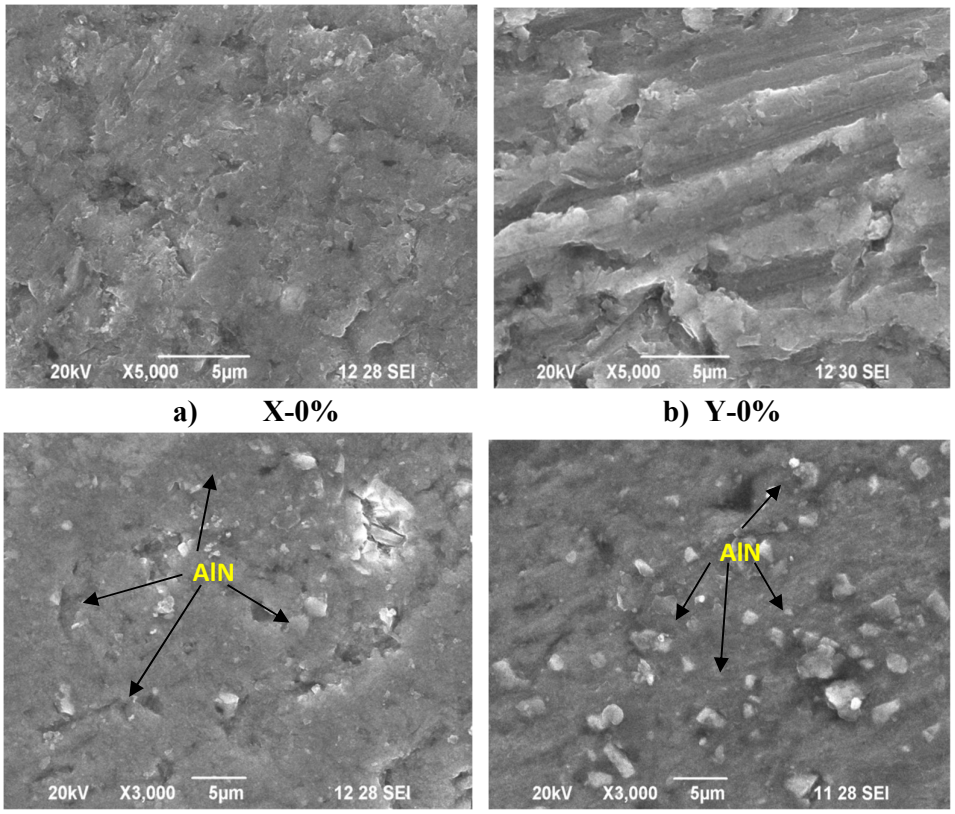

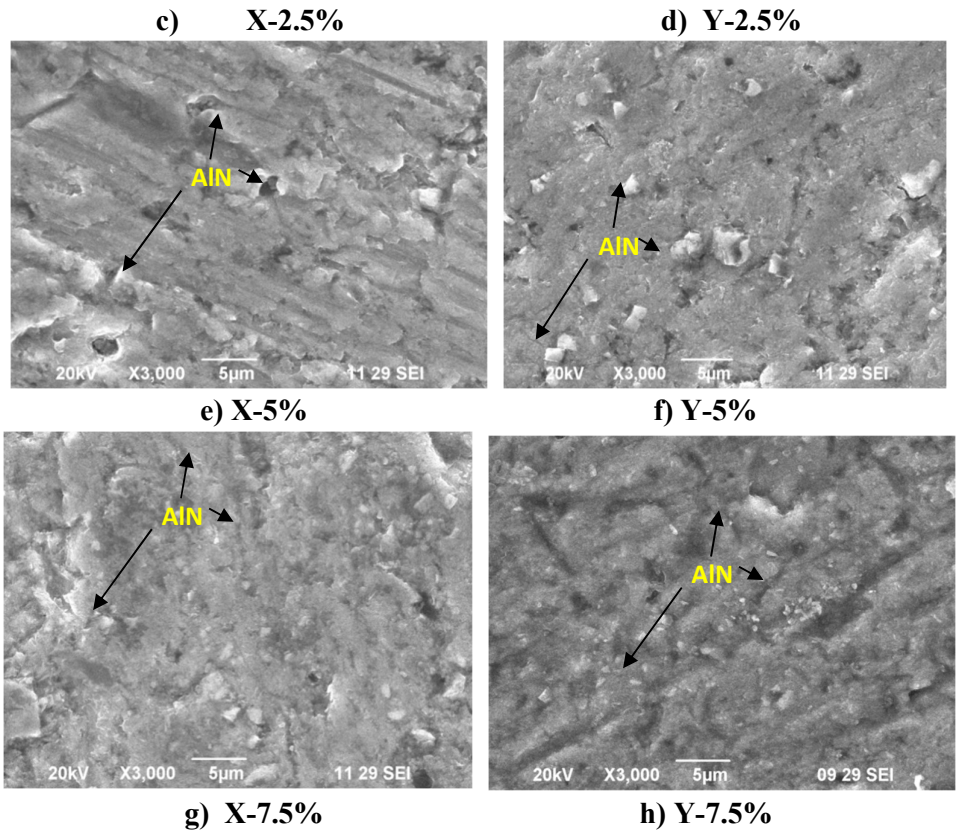

Figure 4 ER4043-AlN composites along the longitude(X) and transverse (Y) direction

Figures 4 (a, c, e, g) show specimens cut in the X (Longitudinal) direction, while Figures 4 (b, d, f, h) show SEM of 0 %, 2.5 %, 5 %, and 7.5 % composites cut in the Y (perpendicular) direction.

The AlN particles are cluster-free and equally joined into the matrix, as shown in Figure 4 (a, c, e, g). WAAM in the reinforcements is also pure, as well as the strengthening of the matrix interactions is visible. Scanning electron micrographs of 0%, 2.5%, 5%, and 7.5% AlN composites in the Y direction are shown in Figure 4(b, d, f, h). The AlN particles are anisotropic, cluster-free, and uniformly united into the matrix, as shown in the micrographs. The WAAM reinforcements are also pure, with clear matrix-reinforcement interactions.

Figure 5 depicts the clear interface between aluminium alloy and AlN, due to the absence of interfacial reaction between the matrix and the reinforcement. Moreover, the addition of absolute ethanol and 99.99% and pure argon gas enhances the weldability between AlN and aluminium alloy matrix, resulting in good bonding between AlN and ER4043 aluminium alloy matrix. Most of the AlN particles are located in intragranular regions. A cluster of AlN particles is seen in a few places. Figure 5(a) to (e) confirms the energy of the 0%, 2.5%, 5%, and 7.5% AlN composite samples in both longitudinal (X) and transverse (Y) directions. The determined EDAX design affirms the presence of the AlN fortifications, notwithstanding the other alloying components present in the composite example.

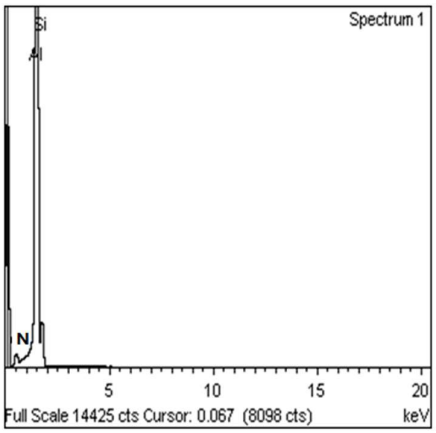

a) X-0%

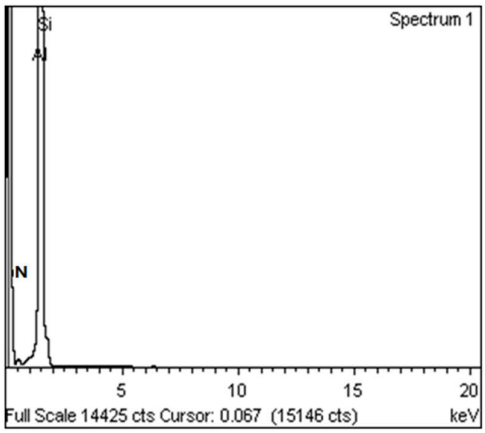

b) Y-0%

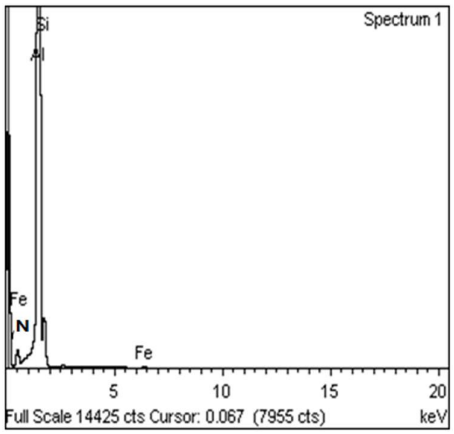

c) X-2.5%

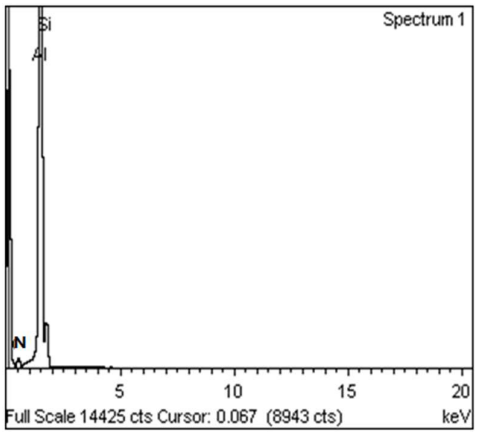

d) Y-2.5%

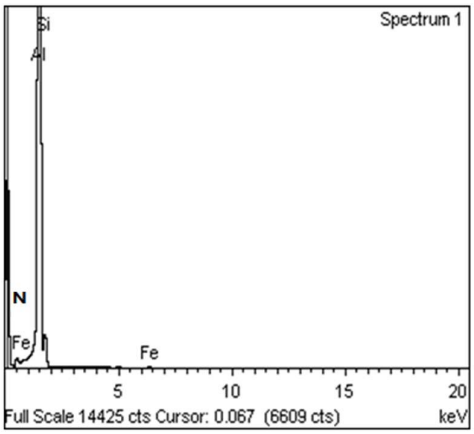

e) X-5%

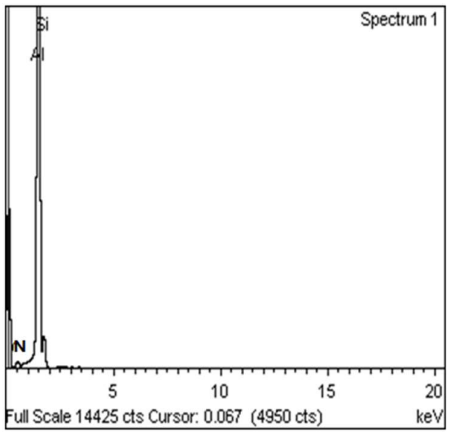

f) Y-5%

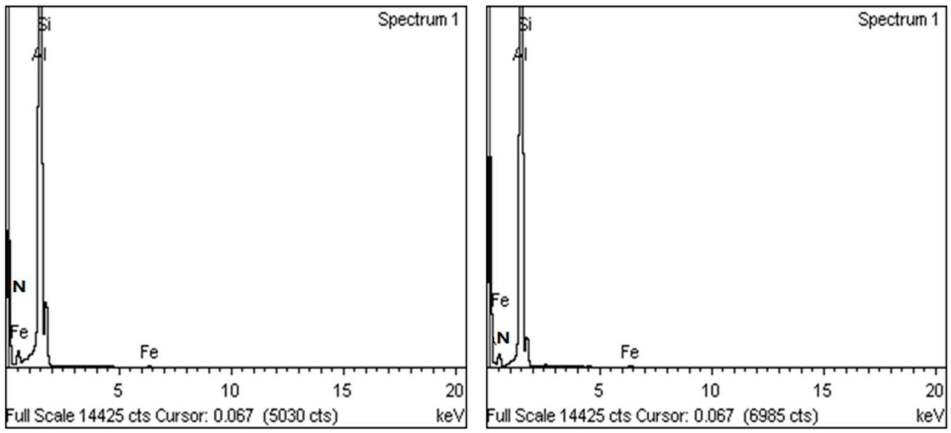

g) X-7.5% **h) Y-7.5%**

Figure 5 Energy-dispersive spectrum of the composites along the X & Y direction.

3.3. Micro-Vickers hardness

It is evident from Figure 7, the microhardness of WAAM composites increased by increasing the reinforcement ratio from 0% to 7.5% AlN for both longitudinal and transverse directions. It is attributed that the increment in the reinforcement ratio increases the strengthening effect. Hence, the higher reinforcement ratio maximizes the hardness [[14] [xxix]]. Further, the traverse specimens have a greater hardness than the longitudinal specimens. It is noted that the WAAM longitudinal specimen has more grain boundaries, while the longitudinal specimen contains more columnar grains [[15] [16] xxx xxxi]. In the first deposited layers, the cold substrate and increased heat dissipation accelerate the rapid cooling rate, resulting in a maximum hardness along the traverse direction [xxxii].

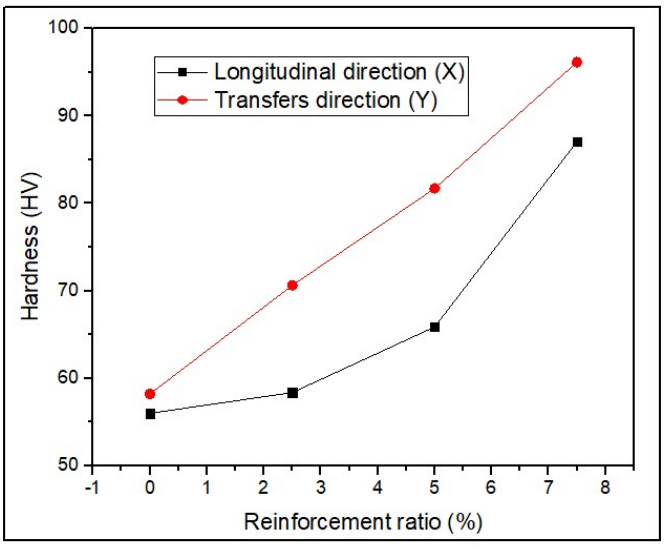

Figure 7 Analysis of Microhardness

4. Conclusion

The current study contributes to the wear behaviour of the ER4043-AlN composite samples under the longitudinal and transverse directions. From the result and analysis, the following

conclusions have arrived. WAAM with MIG welding has successfully produced ER4043-AlN composites. SEM and EDAX validated AlN reinforcements and distribution.

- With the WAAM process, the most homogeneous wall structure height could be produced, i.e., the wall drop at the beginning or end of the structure is the lowest.
- The defect-free structure was fabricated using the WAAM process.
- A strong correlation between the microstructure and the energy input concerning both the grain size and porosity was shown.
- The presence of reinforcements increased the micro-hardness of ER4043-AlN composites, with transverse samples being harder than longitudinal ones.
- Regarding the hardness in the direction of the buildup, a slight influence of the applied arc mode could be determined. This was in the range of 76 HV for the X direction and 64 HV for the Y direction. Accordingly, the hardness increased slightly with the reduced energy input.

The study of wear characteristics in AM is in its infancy. The feasibility of a double-wire system will be investigated in the near future. To quantify the impacts of crystal structure, simulation, postprocess mitigation, fatigue, creep, and corrosion on the overall dimensions and performance of printed components. Improvements in structural stability via process parameter optimization.

References

[i] DebRoy T, Wei HL, Zuback JS, Mukherjee T, Elmer JW, Milewski JO, et al. Additive manufacturing of metallic components – Process, structure and properties. Progress in Materials Science. 2018; 92:112–224.

[ii] David SA, DebRoy T. Current Issues and Problems in Welding Science. Science. 1992; 257(5069):497–502.

[iii] T. DebRoy, S.A. David, Physical processes in fusion welding, Reviews of Modern Physics. 1995, 67 (1) 85.

[iv] Wei HL, Mazumder J, DebRoy T. Evolution of solidification texture during additive manufacturing. Scientific Reports. 2015; 5(1).

[v] Ou W, Mukherjee T, Knapp GL, Wei Y, DebRoy T. Fusion zone geometries, cooling rates and solidification parameters during wire arc additive manufacturing. International Journal of Heat and Mass Transfer. 2018;127:1084–94.

[vi] Dorn, L. Schweißverhalten von Aluminium und seinen Legierungen. Mater. Materialwissenschaft und Werkstotechnik 1998, 29, 412–423.

[vii] Grave, M. Beitrag zum MIG- und WIG-Schweißen von Aluminium legierungen. In Aachener Berichte Fügetechnik; Dilthey, U., Ed.; Shaker Verlag: Düren, Germany, 1998; 3.

[viii] Gierth M, Henckell P, Ali Y, Scholl J, Bergmann JP. Wire Arc Additive Manufacturing (WAAM) of Aluminum Alloy AlMg5Mn with Energy-Reduced Gas Metal Arc Welding (GMAW). Materials. 2020;13(12):2671.

[ix] Gu, J.; Cong, B.; Ding, J.; Williams, S.W.; Zhai, Y. Wire+Arc additive manufacturing of aluminium. In Proceedings of the 25th Annual International Solid Freeform Fabrication Symposium, Austin, TX, USA,4–6 August 2014; Bourell, D.L., Ed.; University of Texas: Austin, TX, USA, 2014.

[x] Williams, S.W.; Martina, F.; Addison, A.C.; Ding, J.; Pardal, G.; Colegrove, P. Wire + Arc Additive Manufacturing. Materials Science and Technology, 2015, 32, 451–458.

[xi] Cong, B.; Ding, J.;Williams, S. Effect of arc mode in cold metal transfer process on porosity of additively manufactured Al-6.3%Cu alloy. The International Journal of Advanced Manufacturing Technology. 2015, 76, 1593–1606.

[xii] Gu, J.; Ding, J.;Williams, S.W.; Gu, H.; Ma, P.; Zhai, Y. The effect of inter-layer cold working and post-deposition heat treatment on porosity in additively manufactured aluminum alloys. Journal of Materials Processing Technology, 2016, 230, 26–34.

[xiii] Hauser T, Reisch RT, Breese PP, Lutz BS, Pantano M, Nalam Y, et al. Porosity in wire arc additive manufacturing of aluminium alloys. Additive Manufacturing. 2021; 41:101993.

[xiv] Fu R, Tang S, Lu J, Cui Y, Li Z, Zhang H, et al. Hot-wire arc additive manufacturing of aluminum alloy with reduced porosity and high deposition rate. Materials & Design. 2021; 199:109370.

[xv] Cong, B.; Qi, Z.; Qi, B.; Sun, H.; Zhao, G.; Ding, J. A Comparative Study of Additively Manufactured Thin Wall and Block Structure with Al-6.3%Cu Alloy Using Cold Metal Transfer Process. Applied Sciences, 2017, 7, 275.

[xvi] Fang, X.; Zhang, L.; Li, H.; Li, C.; Huang, K.; Lu, B. Microstructure Evolution and Mechanical Behavior of 2219 Aluminum Alloys Additively Fabricated by the Cold Metal Transfer Process. Materials 2018, 11, 812.

[xvii] Gu, J.L.; Ding, J.L.; Cong, B.Q.; Bai, J.; Gu, H.M.;Williams, S.W.; Zhai, Y.C. The Influence of Wire Properties on the Quality and Performance of Wire+Arc Additive Manufactured Aluminium Parts. Advanced Materials Research. 2014, 1081, 210–214.

[xviii] Ryan, E.M.; Sabin, T.J.;Watts, J.F.; Whiting, M.J. The influence of build parameters and wire batch on porosity of wire and arc additive manufactured aluminium alloy 2319. Journal of Materials Processing Technology. 2018, 262, 577–584.

[xix] Derekar, K.; Lawrence, J.; Melton, J.; Addison, A.; Zhang, X.; Xu, L. Influence of interpass temperature on wire arc additive manufacturing (WAAM) of aluminium alloy components. In Proceedings of the 71st IIW Annual Assembly and International Conference, Bali, Indonesia, 15–20 June 2018; International Institute of Welding: Bali, Indonesia, 2018.

[xx] Geng, H.; Li, J.; Xiong, J.; Lin, X. Optimisation of interpass temperature and heat input for wire and arc additive manufacturing 5A06 aluminium alloy. Science and Technology of Welding and Joining. 2016, 22, 472–483.

[xxi] Vemanaboina, H., Akella, S., Uma Maheshwer Rao, A., Gundabattini, E., & Buddu, R. K. Analysis of thermal stresses and its effect in the multipass welding process of SS316L. Proceedings of the Institution of Mechanical Engineers, Part E: Journal of Process Mechanical Engineering, 2020, 235(2), 384–391.

[xxii] Cong, B.; Ouyang, R.; Qi, B.; Ding, J. Influence of Cold Metal Transfer Process and Its Heat Input on Weld Bead Geometry and Porosity of Aluminum-Copper Alloy Welds. Rare Metal Materials and Engineering, 2016, 45, 606–611.

[xxiii] Li S, Zhang LJ, Ning J, et al. Microstructures and mechanical properties of Al-Zn-Mg aluminium alloy samples produced by wire + arc additive manufacturing. Journal of Materials Research and Technology, 2020;9(6):13770-13780.

[xxiv] Hamilton JD, Ramesh S, Harrysson OLA, Rock CD, Rivero I V. Cryogenic mechanical alloying of aluminum matrix composites for powder bed fusion additive manufacturing. Journal of Composite Materials, 2021;55(5):641-651.

[xxv] Chen C, Cui C, Zhao L, Liu S, Liu S. The formation mechanism and interface structure characterization of in situ AlN/Al composites. Journal of Composite Materials. 2016; 50(4):495-506.

[xxvi] Fale S, Likhite A, Bhatt J. Compressive, tensile and wear behavior of ex situ Al/AlN metal matrix nanocomposites. . Journal of Composite Materials, 2015; 49(16): 1917 - 1928.
[xxvii] Zhang C, Gao M, Zeng X. Workpiece vibration augmented wire arc additive manufacturing of high strength aluminum alloy. Journal of Materials Processing Technology, 2019; 271:85-92.
[xxviii] Nyhus, B., Dumoulin, S., Nordhagen, H.O., Midling, O.T., Myhr, O.R., Furu, T., Lundberg, S., 2017. Cross-weld tensile strength of aluminum alloys EN AW 5083 and 6082. In: San Francisco, CA, USA, June 25–30. Proc. 27th Int. Ocean and Polar Eng. Conf. IV.pp. 62–70.
[xxix] Natarajan S, Narayanasamy R, Kumaresh Babu SP, Dinesh G, Anil Kumar B, Sivaprasad K. Sliding wear behaviour of Al 6063/TiB2 in situ composites at elevated temperatures. Materials and Design, 2009; 30(7):2521-2531.
[xxx] Shen C, Pan Z, Cuiuri D, Dong B, Li H. In-depth study of the mechanical properties for Fe3Al based iron aluminide fabricated using the wire-arc additive manufacturing process. Materials Science and Engineering: A. 2016;669:118-126.
[xxxi] Qi Z, Qi B, Cong B, Sun H, Zhao G, Ding J. Microstructure and mechanical properties of wire + arc additively manufactured 2024 aluminum alloy components: As-deposited and post heat-treated. Journal of Manufacturing Processes. 2019;40:27-36.
[xxxii] Rodrigues TA, Duarte V, Avila JA, Santos TG, Miranda RM, Oliveira JP. Wire and arc additive manufacturing of HSLA steel: Effect of thermal cycles on microstructure and mechanical properties. Additive Manufacturing. 2019;27:440-450.